Commun. Comput. Chem.
doi: 10.4208/cicc.2016.v4.n2.1

Vol.4, No.2, pp.36-47
Aug. 2016

REGULAR ARTICLE

A theoretical study on the reaction mechanisms and stereoselectivities of NHC-catalyzed [2 + 2] cycloaddition of ketene with C=N double bond of isothiocyanate

Xue Li, Yang Wang, Donghui Wei*, Zhongjun Li

The College of Chemistry and Molecular Engineering, Center of Computational Chemistry, Zhengzhou University, Zhengzhou, Henan Province, 450001, P.R. China

Received 7 Aug 2016; Accepted (in revised version) 30 Aug 2016

Abstract: In this work, three possible mechanisms, including mechanisms A and B associated with the stereoselective [2 + 2] cycloaddition product and mechanism C associated with the [2 + 2 + 2] cycloaddition product, have been investigated for N-heterocyclic carbenes (NHCs) catalyzed cycloadditions of ketenes with isothiocyanates by using density functional theory (DFT). Our calculated results suggest that the mechanism A is the most energy favorable pathway, which contains three steps, i.e. (1) the nucleophilic attack on the ketene by NHC catalyst for the formation of enolate intermediate, (2) regioselective [2 + 2] cycloaddition of the enolate intermediate with isothiocyanate, and (3) the dissociation of the NHC catalyst from the thioxo-β-lactam product. Notably, the [2 + 2] cycloaddition step is proved to be both the rate- and stereoselectivity-determining step. Moreover, the reaction pathway associated with the R configuration is the most favorable pathway and leads to the major product, which is in good agreement with the experimental results. The mechanistic insights obtained in the present study should be valuable for the rational design of more efficient organocatalytic cycloadditons for the synthesis of heterocycle compounds with high selectivities.

AMS subject classifications: 92E99

Keywords: DFT, NHC, [2 + 2] Cycloaddition, Stereoselectivity

1. Introduction

* Corresponding author. *Email address*: donghuiwei@zzu.edu.cn (D. Wei)

In modern synthetic and organic chemistry, it is a critical and challenging goal to design highly stereoselective and region-specific reactions. Notably, organocatalysis is playing more and more important role in asymmetric synthesis. Since the first report of the isolation and characterization of a free N-heterocyclic carbene (NHC), [1] NHCs have been successfully and widely applied as the ligands of organometallic catalysts. [2-5] Afterwards, the excellent performances of NHCs have been uncovered for acting as one of the most powerful organocatalysts in asymmetric reactions, such as the cross-benzoin, Stetter, annulation, homoenolate, [1, 6-16] and cycloaddition (i.e., [2 + 2], [17-22] [2 + 2 + 2], [23] [4 + 2], [24-27] cycloadditions) reactions, which can afford a facile and also effective route to obtain various heterocyclic skeletons. Due to the special reactivities and wide applications of NHC-catalyzed [2 + 2] cycloadditions of ketenes and C = X (X = O, CH2, and NH), their theoretical studies [28-30] have also attracted more and more attention.

Recent reports show that the Lewis base organocatalysts (especially for N-heterocyclic carbenes) can improve the stereoselectivity of the ketene cycloaddition reaction significantly. For instance, the remarkable work of NHC-catalyzed [2 + 2] cycloaddition reactions of ketenes with isothiocyanates (**Scheme 1**) were firstly published by Ye's group. [20] To the best of our knowledge, the reaction mechanisms are still ambiguous, and which step is the stereoselectivity-determining step and which factor is the decisive one for the stereoselectivity in this kind of reaction remain unclear. In this work, we mainly focused on some issues still unsettled: (1) Which reactant (**R1** or **R2**) can react with **Cat** firstly? (2) Which processes are the rate- and stereoselectivity-determining step? (3) Why is the R-isomer the major product? (4) Why does the [2 + 2] cycloaddition rather than other cycloadditions (such as [2 + 2 + 2] cycloaddition) favorably occur? With these questions as motivation, the present work will pursue a theoretical investigation on the title reaction to clarify the actually reaction mechanism and the above questions. And we believe that the mechanistic information should be important for understanding the NHC-catalyzed [2 + 2] cycloaddition reactions and providing novel insights into recognizing this kind of reaction in detail.

In this work, the [2 + 2] cycloaddition of aryl(alkyl)ketene **R1** with PNP-isothiocyanate **R2** promoted by NHC catalyst to give the corresponding major β-lactone **P*R*** (up to 85% yield) with 97% ee (**Scheme 1**) has been chosen as the object of the theoretical investigation. As shown in **Scheme 1**, it should be noted that the "*R*/*S*" represents the chirality of C3 atom in the stationary points involved in the reaction. The reaction mechanisms were studied using density functional theory, which has been widely used in the studies of the reaction mechanisms.

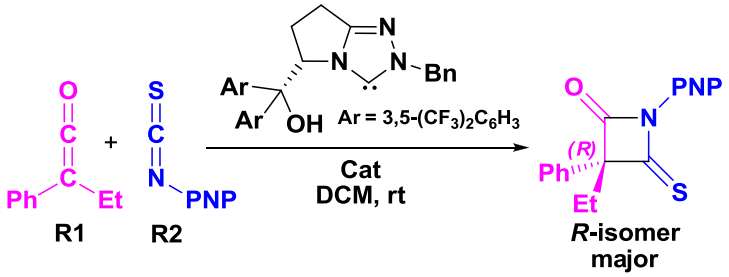

Scheme 1. The NHC-catalyzed [2 + 2] cycloaddition reaction of ketene with isothiocyanate.

2. Computational Details

All structures of the reactants, transition states, intermediates, and products reported in the present study were calculated using the M06-2X [31-33] density functional theory in Gaussian09 [34]. Geometry optimizations were performed using the 6-31G(d,p) basis set [35-36] in the gas phase. The harmonic vibrational frequency calculations were conducted at the same theory level as that used for geometry optimizations to provide thermal corrections of Gibbs free energies. We confirmed that the local minima had no imaginary frequencies, while the saddle points had only one imaginary frequency. The same level of intrinsic reaction coordinate (IRC) [37-38] calculations were performed to confirm that each transition state structure connected with the corresponding reactant and product on the potential energy surface.

On the basis of the optimized structures in the gas phase at the M06-2X/6-31G(d, p) level, the energies were the refined by M06-2X/6-311+G(d, p) single-point calculations with solvent effects (dichloromethane, which was chosen from the available experiment) included and simulated by the integral equation formalism polarizable continuum model (IEF-PCM). [36] In the following parts of this paper, all discussions in this theoretical study are based on solution phase single point energy corrected by gas phase Gibbs free energy correction, i.e. $\Delta E_{discussed} = \Delta E_{SP/solv} + \Delta E_{corr}$, where $\Delta E_{discussed}$, $\Delta E_{SP/solv}$, and ΔE_{corr} represent the energies discussed in text, the solvated single point energy, the corresponding gas-phase Gibbs free energy correction. The computed structures were rendered using the CYLView software [39].

3. Results and Discussions

Base on the experimentally observed products, [20] three possible mechanisms A, B, and C depicted in **Scheme 2** have been considered and investigated in this work. Both mechanisms A and C are initiated by the coordination between **Cat** and **R1**, while the mechanism B is

originated by the reaction between **Cat** and **R2**. For the mechanisms A and B, each has only three steps, including coordination of catalyst and substrate, [2 + 2] cycloaddition, and the regenaration of NHC. With respect to the [2 + 2 + 2] cycloaddition, mechanism C contains four steps in the catalytic cycle, the first step is the same to that of mechanism A, the second step is the nucleophilic attack on **R2**, the third step is the [2 + 2 + 2] cycloaddition, and the eventual step is the dissociation of the products and the catalyst.

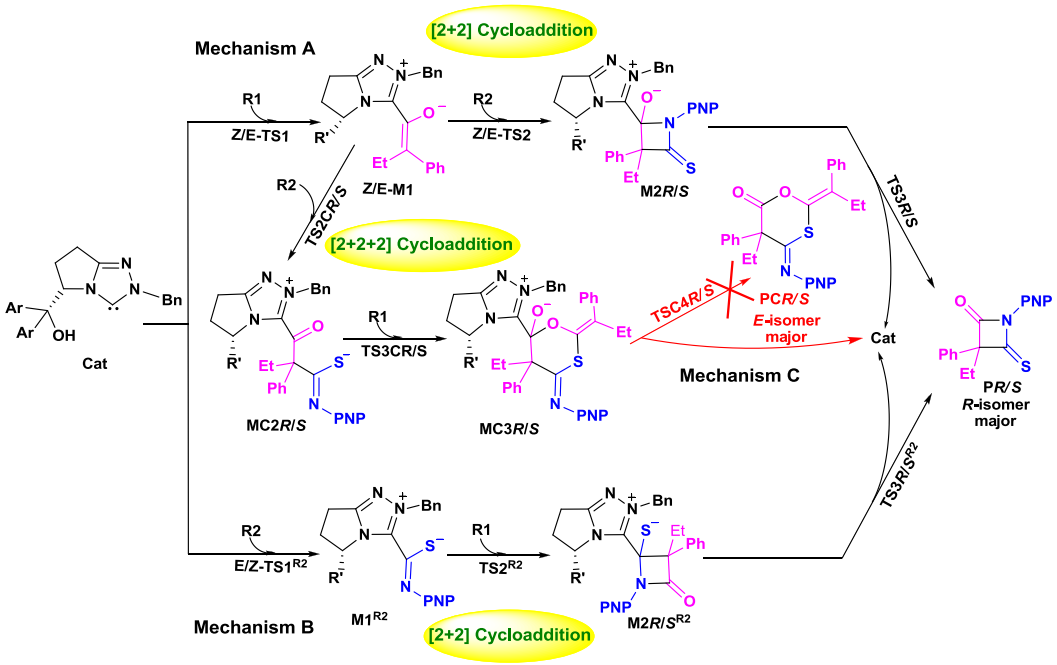

Scheme 2. The possible catalytic cycles for the NHC-catalyzed cycloaddition reactions.

3.1. [2 + 2] Cycloaddition Reaction Mechanisms A and B

In this reaction, the NHC catalyst **Cat** catalyzed [2 + 2] cycloaddition reaction mechanisms (Mechanisms A and B) of ketene (**R1**) with isothiocyanate (**R2**) are investigated.

3.1.1. Step 1: Nucleophilic attack of Cat on reactant.

For mechanism A, the catalyst **Cat** initially interacts with **R1** to form the Z/E-configurational pre-intermediate **M0** (denoted as **Z/E-M0**), in which the "Z/E" represents the Z/E-configuration of the C3=C4 double bond. Then, as shown in **Scheme 2**, the C1 atom in **Cat** nucleophilically attacks on the C4 atom in **R1** to afford intermediate **Z/E-M1** via transition state **Z/E-TS1,** respectively**. Figure 1** shows that the distance of the C1–C4 bond reduces from 2.47/2.42 Å in **Z/E-TS1** to 1.50/1.50 Å in **Z/E-M1**, which implies the complete

coordination of **Cat** with **R1**. **Figure 2** exhibits the Gibbs free energy profile for the whole reaction, in which the energies of **Cat**+**R1**+**R2** were set as the reference of 0.0 kcal/mol. Moreover, **Z/E-M0** and **Z/E-TS1** locate 11.15/7.13 and 18.60/16.95 kcal/mol above the reactants in energy, while **Z/E-M1** locates -9.46/-12.21 kcal/mol below the reactants in energy.

For mechanism B, **Cat** firstly interacts with **R2** rather than **R1** to form intermediate **M0^{R2}**. Namely, the nucleophilic attack by the C1 of **Cat** on the C7 of **R2** leads to the formation of C1–C7 bond in the **M1^{R2}** intermediate via the **TS1^{R2}** transition state**.** The distance of C1–C7 bond presented in **Figure 1** is shortened form 2.27 Å in **TS1^{R2}** to 1.49 Å in **M1^{R2}**, implying the complete coordination of **Cat** with **R2**. The ΔG of **M0^{R2}**, **TS1^{R2}** and **M1^{R2}** are 9.32, 23.62 and -9.41 kcal/mol respectively, thus, the energy barrier of this pathway is obviously higher than that of mechanism A, suggesting the nucleophilic attack of **Cat** to **R2** is relatively unpreferred.

3.1.2. Step 2: [2 + 2] cycloaddition.

The second step is to accomplish the [2 + 2] cycloaddition of **Z/E-M1** with **R2** (mechnism A), or that of **M1^{R2}** with **R1** (machanism B). As illustrated in **Scheme 2**, there is only one possible addition pattern in mechanism A, which is due to the bulky substituent of Ar (Ar = 3,5-(C_3F_3)$_2$$C_6H_3$). Since the ketene **R2** could only attack to the *Re* face of **Z-M1** and the *Si* face of **E-M1**, resulting in the formation of two chemical bonds C3–C7 and C4–N6 in intermediate **M2** via the transition state **TS2**. Meanwhile, two chiral carbons C3 and C4 are formed in **M2**, namely, the **M2** is associated with the two configurations **(Z-)M2*RR*** and **(E-)M2*SR*** (where the "*R*" or "*S*" represents the chiralities of the C3 and C4 atoms, respectively), but the chirality of the C4 atom would disappear in the following dissociation step. As depicted in **Figure 1**, the distances of C3–C7 and C4–N6 are 2.03/2.19 Å and 2.66/2.58 Å in **TS2*R*/*S*** and 1.53/1.53 Å and 1.51/1.51 Å in **M2*R*/*S***, separately. The optimized geometries of the two transition states suggest that the C3–C7 and C4–N6 bonds are formed asynchronously, and formation of the C3–C7 bond goes earlier than that of the C4–N6 bond. In another word, the [2 + 2] cycloaddition occurs in a concerted but asynchronous manner.

As mentioned above, there are two chiral carbon centers (C3 and C4) generated in the [2 + 2] cycloaddition process. However, the new formation C4 chiral carbon center disappears in products, while the other C3 chiral carbon center still exists in products. As shown in **Figure 2**, the energy barrier via **TS2*R*/*S*** is 24.45/29.74 kcal/mol, indicating the pathway associated with **TS2*R*** has the lower energy barrier between the two competing pathways, thus, it should be the more favorable pathway and the *R* configuration would be the major stereoisomer, which is in agreement with the experiment. Obviously, the energy barrier via **TS2*S*** is remarkably higher than that via **TS2*R***, so the mechanism discussion on the *S*-configuration can be ignored in the following part.

Considering the [2 + 2] cycloaddition of **M1**^{R2} with **R1** in mechanism B, there are two possible addition patterns which correspond to two configurations of the cycloadducts as shown in **Scheme 2**. Since the ketene **R1** could attack to either the Re or Si face of **M1**^{R2}, leading to the two same chemical bond formations of C3–C7 and C4–N6 in intermediate **M2***R*/*S*^{R2} via the transition state **TS2***R*/*S*^{R2}. The barriers of 36.77/38.57 kcal/mol via **TS2***R*/*S*^{R2} are much higher, suggesting the process is impossible to happen under the experimental conditions (the room temperature), so the mechanism B should be excluded. That is to say, the nucleophilic attack only happens via mechanism A**.**

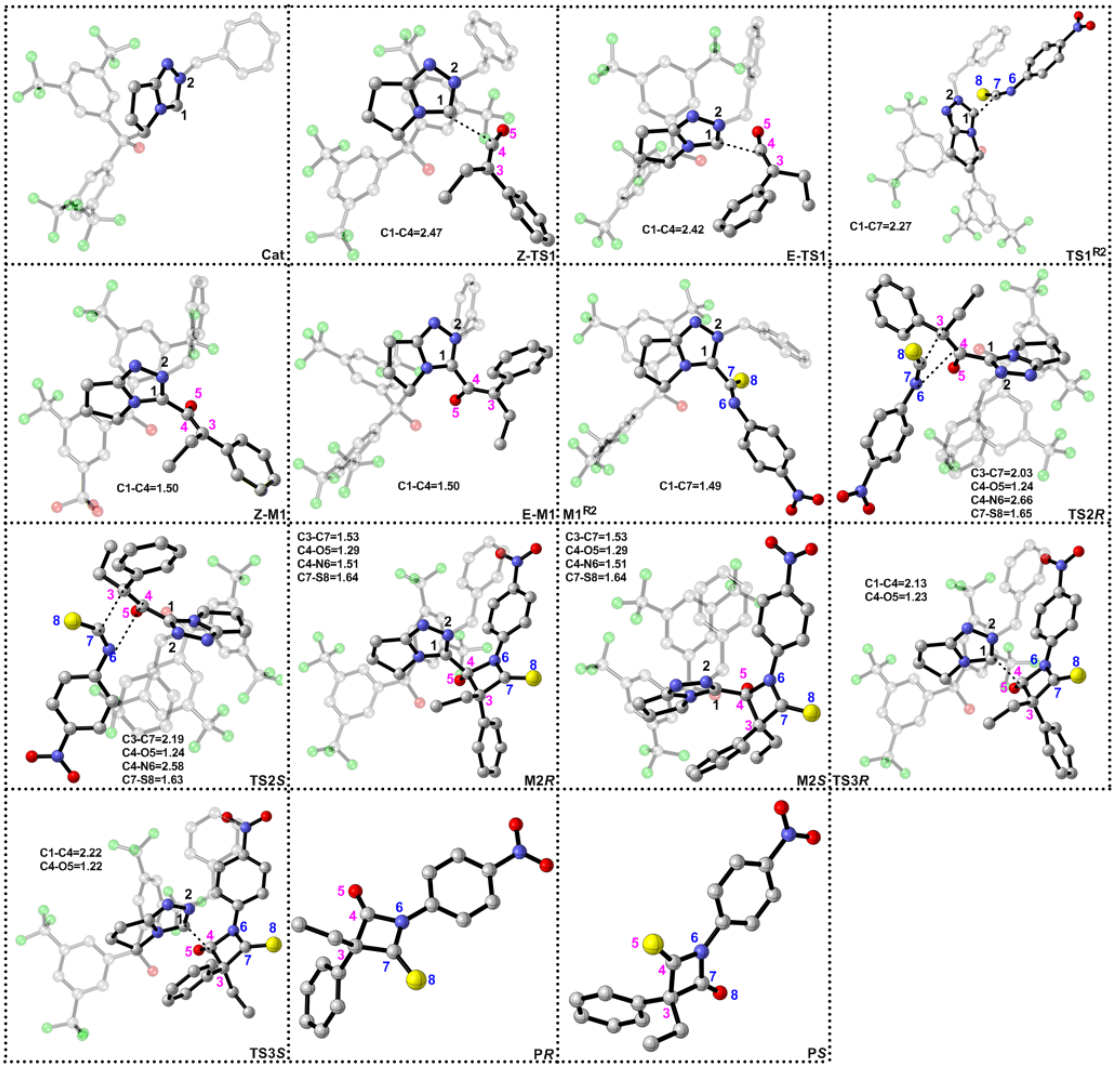

Figure 1: Optimized geometries of the stationary points involved in NHC-catalyzed [2 + 2] cycloaddition. All distances are given in Å and all the hydrogens are omitted for the sake of clarity.

3.1.3. Step 3: Regeneration of the catalyst.

As aforementioned, the pathway for the formation of the *R*-configuration major product (**P*R***, **Scheme 2**) in mechanism A is more energetically favorable than that of the *S*-configuration minor one (**P*S***, **Scheme 2**) as shown in **Figure 2**. Therefore, we only discuss the product **P*R*** formation step. As presented in **Scheme 2**, the catalyst NHC is dissociated with product **P*R*** by breaking the C1–C4 bond through transition state **TS3*R***, and the change of the distance C1–C4 reflects the nature of the last step in mechanism A. The distance C1–C4 is lengthened to 2.13 Å in **TS3*R***. The energy of **M3*R*** is 4.68 kcal/mol lower than those of the reactants, indicating the overall reaction is an exothermic process. Furthermore, the energy barrier via **TS3*R*** is 13.77 kcal/mol, demonstrating that the third step should be a fast process, and it is easy to regenerate the catalyst **Cat** and form the corresponding major product **P*R***.

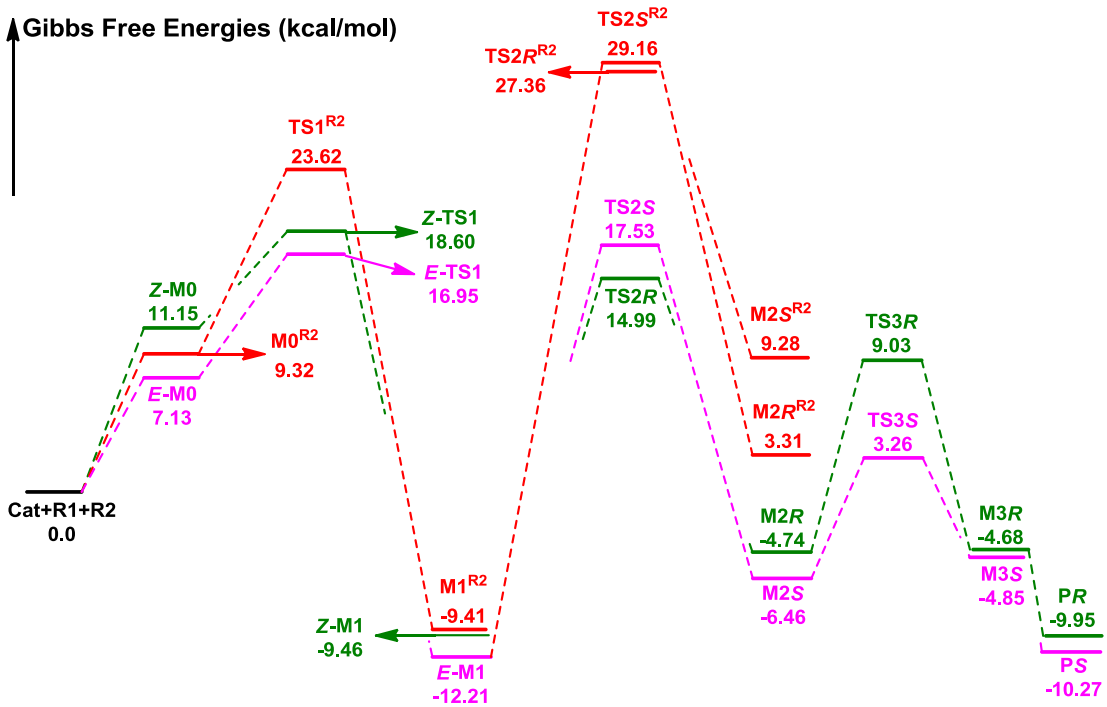

Figure 2: The Gibbs free energy profile of **Cat**-catalyzed [2 + 2] cycloaddition reaction of ketene with isothiocyanate.

As discussed above, the mechanism A is the most favorable pathway. Comparing the three energy barriers of 7.45, 24.45 and 13.77 kcal/mol via the corresponding transition states **Z-TS1**, **TS2*R*** and **TS3*R***, we know the second step (i.e. [2 + 2] cycloaddition) has the highest energy barrier, implying this process is also the rate-determining step.

3.2. [2 + 2 + 2] Cycloaddition Reaction Mechanism C

In this part, the NHC catalyst **Cat** catalyzed [2 + 2 + 2] cycloaddition reaction mechanism C (in **Scheme 2**) is also explored. As depicted in **Scheme 2**, the mechanism C is diverged with mechanism A from the intermediate **Z/E-M1**, so we start the discussion of the mechanism C from the second step.

As we can see in **Scheme 2**, for the second step of the mechanism C, the previous formed intermediate **Z/E-M1** nucleophilically attacks on the *Re* or *Si* face of isothiocyanate **R2** to afford the intermediate **MC2*R*/*S*** via the transition state **TSC2*R*/*S*** respectively, which is accompanied with the formation of one chiral carbon center**.** The barriers of 32.78/27.76 kcal/mol via **TSC2*R*/*S*** are obviously higher than those of mechanism A, indicating the [2 + 2 + 2] cycloaddition process is not preferred to occur at the room temperature, which is in agreement with the experiment, so the mechanism C should be directly excluded.

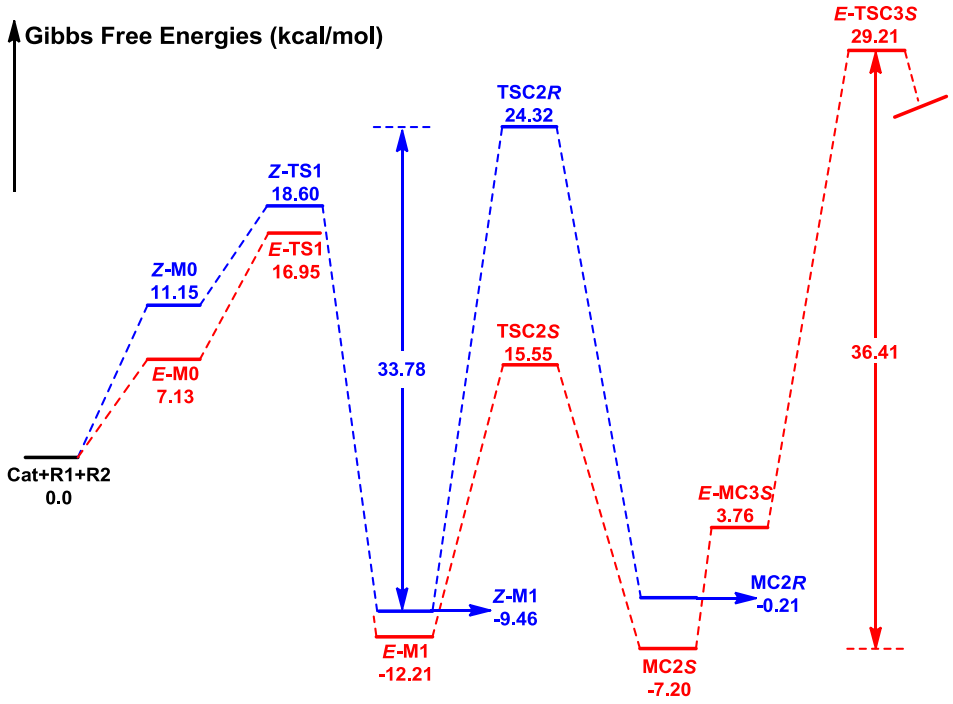

Figure 3: The Gibbs free energy profile of **Cat**-catalyzed [2 + 2 + 2] cycloaddition reaction of ketenes with isothiocyanate.

4. Conclusion

In this paper, the possible mechanisms and stereoselectivities for the NHC-catalyzed [2 + 2] and [2 + 2 + 2] cycloaddition reactions of ketenes and isothiocyanates have been investigated

using density functional theory (DFT). We have discussed and investigated the three mechanisms A, B and C of the NHC-catalyzed cycloaddition reactions to generate two kinds of stereoisomers. The calculated results reveal that the favorable mechanism A involves three steps. Initially, NHC approaches the carbonyl group of the ketene. The second step is a [2 + 2] cycloaddition process, which can lead to two kinds of configurational intermediates via different diastereotopic transition states. The remaining step involves the dissociation of catalyst NHC and the product. Moreover, the [2 + 2] cycloaddition step is calculated to be both the rate-determining and stereoselectivity-determining step, and the energy barriers corresponding to the stereoisomer transition states **TS2*R*/*S*** are 24.45 and 29.74 kcal/mol, respectively. The energetic favorability of the *R* configuration stereoisomer suggests that it should be the dominant product, which is in good agreement with the experiment. That is to say, the transition state associated with the second step should be the key for the stereoselectivity of the title reaction. In summary, this study provides a theoretical model for predicting the stereoselectivity of the product, which should be helpful for rational design of potent catalysts to synthesize thioxo-β-lactams with high stereoselectivity.

Acknowledgments

The work described in this paper was supported by the National Natural Science Foundation of China (No. 21303167), China Postdoctoral Science Foundation (Nos. 2013M530340 and 2015T80776), Outstanding Young Talent Research Fund of Zhengzhou University (No.1521316001), and Excellent Doctoral Dissertation Engagement Fund of Zhengzhou University in 2014.

Reference

[1] A. J. Arduengo, R. L. Harlow and M. Kline, A stable crystalline carbene. J. Am. Chem. Soc., 113 (1991), 361-363.

[2] G. C. Fortman and S. P. Nolan, N-Heterocyclic carbene (NHC) ligands and palladium in homogeneous cross-coupling catalysis: a perfect union. Chem. Soc. Rev., 40 (2011), 5151-5169.

[3] R. H. Crabtree, NHC ligands versus cyclopentadienyls and phosphines as spectator ligands in organometallic catalysis. J. Organomet. Chem., 690 (2005), 5451-5457.

[4] V. Lillo, A. Prieto, A. Bonet, M. M. Díaz-Requejo, J. Ramirez, P. J. Pérez and E. Fernández, Asymmetric β-boration of α, β-unsaturated esters with chiral (NHC) Cu catalysts. Organometallics, 28 (2008), 659-662.

[5] P. S. Engl, A. Fedorov, C. Copéret and A. Togni, N-Trifluoromethyl NHC Ligands Provide Selective Ruthenium Metathesis Catalysts. Organometallics, 35 (2016), 887-893.

[6] S. J. Ryan, L. Candish and D. W. Lupton, N-Heterocyclic carbene-catalyzed (4 + 2)

cycloaddition/decarboxylation of silyl dienol ethers with α, β-unsaturated acid fluorides. J. Am. Chem. Soc., 133 (2011), 4694-4697.

[7] T. Y. Jian, L. He, C. Tang and S. Ye, N-Heterocyclic Carbene Catalysis: Enantioselective Formal [2 + 2] Cycloaddition of Ketenes and N-Sulfinylanilines. Angew. Chem. Int. Ed., 50 (2011), 9104-9107.

[8] E. M. Phillips, M. Wadamoto, A. Chan and K. A. Scheidt, A Highly Enantioselective Intramolecular Michael Reaction Catalyzed by N-Heterocyclic Carbenes. Angew. Chem. Int. Ed., 46 (2007), 3107-3110.

[9] D. Enders, A. Grossmann, J. Fronert and G. Raabe, N-heterocyclic carbene catalysed asymmetric cross-benzoin reactions of heteroaromatic aldehydes with trifluoromethyl ketones. Chem. Commun., 46 (2010), 6282-6284.

[10] T. Ema, Y. Oue, K. Akihara, Y. Miyazaki and T. Sakai, Stereoselective synthesis of bicyclic tertiary alcohols with quaternary stereocenters via intramolecular crossed benzoin reactions catalyzed by N-heterocyclic carbenes. Org. Lett., 11 (2009), 4866-4869.

[11] D. A. DiRocco and T. Rovis, Catalytic asymmetric intermolecular Stetter reaction of enals with nitroalkenes: enhancement of catalytic efficiency through bifunctional additives. J. Am. Chem. Soc., 133 (2011), 10402-10405.

[12] T. Jousseaume, N. E. Wurz and F. Glorius, Highly Enantioselective Synthesis of α-Amino Acid Derivatives by an NHC-Catalyzed Intermolecular Stetter Reaction. Angew. Chem. Int. Ed., 50 (2011), 1410-1414.

[13] Q. Kang and Y. G. Zhang, N-Heterocyclic carbene-catalyzed aza-Michael addition. Org. Biomol. Chem., 9 (2011), 6715-6720.

[14] A. Lee and K. A. Scheidt, N-Heterocyclic carbene-catalyzed enantioselective annulations: a dual activation strategy for a formal [4 + 2] addition for dihydrocoumarins. Chem. Commun., 51 (2015), 3407-3410.

[15] H. Lu, J. Y. Liu, C. G. Li, J. B. Lin, Y. M. Liang and P. F. Xu, A new chiral C1-symmetric NHC-catalyzed addition to α-aryl substituted α, β-disubstituted enals: enantioselective synthesis of fully functionalized dihydropyranones. Chem. Commun., 51 (2015), 4473-4476.

[16] X. K. Chen, X. Q. Fang and Y. R. Chi, cis-Enals in N-heterocyclic carbene-catalyzed reactions: distinct stereoselectivity and reactivity. Chem. Sci., 4 (2013), 2613-2618.

[17] X. N. Wang, P. L. Shao, H. Lv and S. Ye, Enantioselective Synthesis of β-Trifluoromethyl-β-lactones via NHC-Catalyzed Ketene−Ketone Cycloaddition Reactions. Org. Lett., 11 (2009), 4029-4031.

[18] X. L. Huang, X. Y. Chen and S. Ye, Enantioselective synthesis of aza-β-lactams via NHC-catalyzed [2 + 2] cycloaddition of ketenes with diazenedicarboxylates. J. Org. Chem., 74 (2009), 7585-7587.

[19] J. Douglas, J. E. Taylor, G. Churchill, A. M. Z. Slawin and A. D. Smith, NHC-Promoted asymmetric β-lactone formation from arylalkylketenes and electron-deficient benzaldehydes or pyridinecarboxaldehydes. J. Org. Chem., 78 (2013), 3925-3938.

[20] X. N. Wang, L. T. Shen and S. Ye, NHC-catalyzed enantioselective [2 + 2] and [2 + 2 + 2]

cycloadditions of ketenes with isothiocyanates. Org. Lett., 13 (2011), 6382-6385.

[21] T. Wang, X. L. Huang and S. Ye, Enantioselective formal [2 + 2] cycloaddition of ketenes with nitroso compounds catalyzed by N-heterocyclic carbenes. Org. Biomol. Chem., 8 (2010), 5007-5011.

[22] H. M. Zhang, Z. H. Gao and S. Ye, Bifunctional N-Heterocyclic Carbene-Catalyzed Highly Enantioselective Synthesis of Spirocyclic Oxindolo-β-lactams. Org. Lett., 16 (2014), 3079-3081.

[23] X. N. Wang, L. T. Shen and S. Ye, Enantioselective [2 + 2 + 2] cycloaddition of ketenes and carbon disulfide catalyzed by N-heterocyclic carbenes. Chem. Commun., 47 (2011), 8388-8390.

[24] Y. Wang, L. J. Zheng, D. H. Wei and M. S. Tang, A quantum mechanical study of the mechanism and stereoselectivity of the N-heterocyclic carbene catalyzed [4 + 2] annulation reaction of enals with azodicarboxylates. Org. Chem. Front., 2 (2015), 874-884.

[25] S. M. Leckie, T. B. Brown, D. Pryde, T. Lebl, A. M. Z. Slawin and A. D. Smith, NHC-mediated enantioselective formal [4 + 2] cycloadditions of alkylarylketenes and β,γ-unsaturated α-ketocarboxylic esters and amides. Org. Biomol. Chem., 11 (2013), 3230-3246.

[26] T. Y. Jian, X. Y. Chen, L. H. Sun and S. Ye, N-heterocyclic carbene-catalyzed [4 + 2] cycloaddition of ketenes and 3-aroylcoumarins: highly enantioselective synthesis of dihydrocoumarin-fused dihydropyranones. Org. Biomol. Chem., 11 (2013), 158-163.

[27] T. Y. Jian, P. L. Shao and S. Ye, Enantioselective [4 + 2] cycloaddition of ketenes and 1-azadienes catalyzed by N-heterocyclic carbenes. Chem. Commun., 47 (2011), 2381-2383.

[28] D. H. Wei, Y. Y. Zhu, C. Zhang, D. Z. Sun, W. J. Zhang and M. S. Tang, A DFT study on enantioselective synthesis of aza-β-lactams via NHC-catalyzed [2 + 2] cycloaddition of ketenes with diazenedicarboxylates. J. Mol. Catal. A: Chem., 334 (2011), 108-115.

[29] M. M. Zhang, D. H. Wei, Y. Wang, S. J. Li, J. F. Liu, Y. Y. Zhu and M. S. Tang, DFT study on the reaction mechanisms and stereoselectivities of NHC-catalyzed [2 + 2] cycloaddition between arylalkylketenes and electron-deficient benzaldehydes. Org. Biomol. Chem., 12 (2014), 6374-6383.

[30] Y. Wang, D. H. Wei, Z. Y. Li, Y. Y. Zhu and M. S. Tang, DFT Study on the Mechanisms and Diastereoselectivities of Lewis Acid-Promoted Ketene–Alkene [2 + 2] Cycloadditions: What is the Role of Lewis Acid in the Ketene and C= X (X= O, CH_2, and NH)[2 + 2] Cycloaddition Reactions? J. Phys. Chem. A, 118 (2014), 4288-4300.

[31] W. J. Zhang, D. G. Truhlar and M. S. Tang, Tests of exchange-correlation functional approximations against reliable experimental data for average bond energies of 3d transition metal compounds. J. Chem. Theor. Comp., 9 (2013), 3965-3977.

[32] Y. Zhao and D. G. Truhlar, Density functionals with broad applicability in chemistry. Acc. Chem. Res., 41 (2008), 157-167.

[33] P. E. M. Siegbahn and M. R. A. Blomberg, Energy diagrams for water oxidation in photosystem II using different density functionals. J. Chem. Theor. Comp., 10 (2013), 268-272.

[34] M. J. Frisch, G. W. Trucks, H. B. Schlegel, G. E. Scuseria, M. A. Robb, J. R. Cheeseman, G. Scalmani, V. Barone, B. Mennucci, G. A. Petersson, H. Nakatsuji, M. Caricato, X. Li, H. P. Hratchian, A. F. Izmaylov,

J. Bloino, G. Zheng, J. L. Sonnenberg, M. Hada, M. Ehara, K. Toyota, R. Fukuda, J. Hasegawa, M. Ishida, T. Nakajima, Y. Honda, O. Kitao, H. Nakai, T. Vreven, J. A. Montgomery, J. E. P. Jr., F. Ogliaro, M. Bearpark, J. J. Heyd, E. Brothers, K. N. Kudin, V. N. Staroverov, T. Keith, R. Kobayashi, J. Normand, K. Raghavachari, A. Rendell, J. C. Burant, S. S. Iyengar, J. Tomasi, M. Cossi, N. Rega, J. M. Millam, M. Klene, J. E. Knox, J. B. Cross, V. Bakken, C. Adamo, J. Jaramillo, R. Gomperts, R. E. Stratmann, O. Yazyev, A. J. Austin, R. Cammi, C. Pomelli, J. W. Ochterski, R. L. Martin, K. Morokuma, V. G. Zakrzewski, G. A. Voth, P. Salvador, J. J. Dannenberg, S. Dapprich, A. D. Daniels, O. Farkas, J. B. Foresman, J. V. Ortiz, J. Cioslowski and D. J. Fox, Gaussian 09, Revision C. 01, Gaussian, Inc., Wallingford CT, 2010.

[35] W. Sang Aroon and V. Ruangpornvisuti, Determination of aqueous acid-dissociation constants of aspartic acid using PCM/DFT method. Int. J. Quantum. Chem., 108 (2008), 1181-1188.

[36] J. Tomasi, B. Mennucci and E. Cances, The IEF version of the PCM solvation method: an overview of a new method addressed to study molecular solutes at the QM ab initio level. J. Mol. Struct.: THEOCHEM, 464 (1999), 211-226.

[37] C. Gonzalez and H. B. Schlegel, An improved algorithm for reaction path following. J. Chem. Phys., 90 (1989), 2154-2161.

[38] C. Gonzalez and H. B. Schlegel, Reaction path following in mass-weighted internal coordinates. J. Phys. Chem., 94 (1990), 5523-5527.

[39] C. Y. Legault, CYLview, v 1.0b, Universite de Sherbrooke, http://www.cylview.org., 2009.